Biochemical and Biophysical Research Communications 454 (2014) 465–470

Contents lists available at ScienceDirect

Biochemical and Biophysical Research Communications

journal homepage: www.elsevier.com/locate/ybbrc

Inhibition of PKM2 sensitizes triple-negative breast cancer cells to doxorubicin

Feng Wang [a,b], Yong Yang [b,c,*]

[a] Department of Gastroenterology, The Tenth People's Hospital of Shanghai, Tongji University, Shanghai 200072, People's Republic of China
[b] Department of Nanomedicine, Houston Methodist Research Institute, Houston, TX 77030, USA
[c] Department of Medicine, Weill Cornell Medical College, New York, NY 10065, USA

ARTICLE INFO

Article history:
Received 16 October 2014
Available online 29 October 2014

Keywords:
Chemotherapy
Pyruvate kinase isoenzyme M2
Glycolysis
Triple-negative breast cancer

ABSTRACT

Cancer cells alter regular metabolic pathways in order to sustain rapid proliferation. One example of metabolic remodeling in cancerous tissue is the upregulation of pyruvate kinase isoenzyme M2 (PKM2), which is involved in aerobic glycolysis. Indeed, PKM2 has previously been identified as a tumor biomarker and as a potential target for cancer therapy. Here, we examined the effects of combined treatment with doxorubicin and anti-PKM2 small interfering RNA (siRNA) on triple-negative breast cancer (TNBC). The suppression of PKM2 resulted in changes in glucose metabolism, leading to decreased synthesis of adenosine triphosphate (ATP). Reduced levels of ATP resulted in the intracellular accumulation of doxorubicin, consequently enhancing the therapeutic efficacy of this drug in several triple-negative breast cancer cell lines. Furthermore, the combined effect of PKM2 siRNA and doxorubicin was evaluated in an *in vivo* MDA-MB-231 orthotopic breast cancer model. The siRNA was systemically administered through a polyethylenimine (PEI)-based delivery system that has been extensively used. We demonstrate that the combination treatment showed superior anticancer efficacy as compared to doxorubicin alone. These findings suggest that targeting PKM2 can increase the efficacy of chemotherapy, potentially providing a new approach for improving the outcome of chemotherapy in patients with TNBC.

1. Introduction

Approximately 20% of all breast cancers are classified as triple-negative, which entails the absence of the estrogen receptor (ER), the progesterone receptor (PR), and the human epidermal growth factor receptor 2 (HER2) [1,2]. This type of breast cancer displays highly proliferative and aggressive characteristics, consequently resulting in poor prognosis [3,4]. In addition, triple-negative breast cancer (TNBC) patients are forced to rely on chemotherapeutics (e.g. doxorubicin), since receptor-targeted and hormonal therapies are of little use. Unfortunately, chemotherapy frequently fails in the treatment of TNBC due to the development of drug resistance [5,6]. Therefore, there exists a pressing need to generate therapeutic strategies that resensitize TNBC cells to cytotoxic drugs. In order to develop such strategies it is important to understand the mechanisms by which cancer cells lose sensitivity to chemotherapy. Genes that are frequently overexpressed in TNBC may provide indications as to which cell-signaling pathways are responsible for circumventing chemotherapy-induced cell death.

Pyruvate kinase isoenzyme M2 (PKM2) is an example of a protein that is widely overexpressed in TNBC cells [7–9]. This enzyme catalyses the final step of glycolysis, resulting in the conversion of phosphoenolpyruvate (PEP) to pyruvate, which generates adenosine triphosphate (ATP) (Fig. S1) [10,11]. Previous reports have shown that the suppression of PKM2 can inhibit tumor growth [7,12]. However, the effect of PKM2 on chemotherapeutic efficacy has not previously been evaluated. In this study we assessed whether PKM2 inhibition could enhance the efficacy of doxorubicin *in vitro* and *in vivo*. The suppression of PKM2 was achieved through systemic administration of siRNA using the polyethylenimine (PEI)-based delivery system, which has been extensively characterized and studied [13–17].

2. Materials and methods

2.1. Cell culture and siRNA transfection

Cell lines were obtained from ATCC. MDA-MB-231 and MDA-MB-436 triple-negative breast cancer cells were cultured in

* Corresponding author at: Department of Nanomedicine, Houston Methodist Research Institute, Houston, TX 77030, USA.
E-mail address: yyang@houstonmethodist.org (Y. Yang).

http://dx.doi.org/10.1016/j.bbrc.2014.10.109
0006-291X/

Dulbecco's Modified Eagle Medium (DMEM, Invitrogen) with 10% fetal bovine serum (FBS, Hyclone). BT-549, BT-20 and HCC70 triple-negative breast cancer cells were cultured in RPMI-1640 (Invitrogen) with 10% FBS. The cell lines were transfected with control siRNA (siControl) and two variants of PKM2 siRNA (siPKM2_1 and siPKM2_2) using oligofectamine (Life Technologies). siRNA oligos were synthesized by Sigma. The sense strand sequences of the siRNAs were: siControl (CUUACGCUGAGUACUUCGA), siPKM2_1 (CCAUAAUCGUCCUCACCAA), and PKM2_2 (GCCAUAAUCGU CCUCACCA).

2.2. Proliferation assay

Cells were transfected for 48 h, after which they were replated and allowed to adhere for 24 h. The cells were then exposed to various concentrations of doxorubicin (Sigma) for 72 h, throughout which the medium was replaced every 24 h to sustain constant levels of doxorubicin and nutrients. The number of cells present at the end of the treatment period was calculated using a Coulter Counter (Beckman). Oligomycin experiments were performed as stated above, with the exception of using cell culture media supplemented with oligomycin (Sigma, 1 ng/mL). The results were normalized to that of control cells expressing the target siRNAs in the absence of doxorubicin. The half maximal inhibitory concentration (IC_{50}) values were analyzed using GraphPad Prism 5.01 software (GraphPad Software Inc.).

2.3. Quantitative reverse transcription polymerase chain reaction (RT-PCR)

Quantitative RT-PCR was carried out as previously described [18]. RNA was extracted from the cells using an RNeasy kit (QIAGEN). Total RNA (1 mg) was reverse transcribed into cDNA with Superscript III from Invitrogen in a 25 ml reaction. Glyceraldehyde 3-phosphate dehydrogenase (GAPDH) served as an endogenous control. The following primer pairs were used:

PKM2 primers: forward primer: 5′-ATTATTTGAGGAACTCC GCCGCCT-3′; reverse primer: 5′-ATTCCGGGTCACAGCAATGATG G-3′.

GAPDH primers: forward primer: 5′-TTCACCACCATGGAGAA GGC-3′; reverse primer: 5′-GGCATGGACTGTGGTCATGA-3′.

2.4. Immunoblotting

The cells were treated with siControl, siPKM2_1 or siPKM2_2 for 72 h. The transfected cells were the lysed with the M-PER mammalian protein transfection reagent (Thermo Scientific) with added protease inhibitors. Following centrifugation of the lysates, the protein concentration in the supernatant was measured using a BCA Protein Assay Kit. The antibodies were diluted in 5% dry milk in Tris-buffered saline (0.1% Tween-20). The PKM2, GAPDH, and horseradish peroxidase (HRP)-conjugated antibodies (Cell Signaling) were used at a dilution of 1:1000, 1:3000, and 1:5000, respectively. The primary antibodies were incubated for 12 h at 4 °C, while the horseradish peroxidase (HRP)-conjugated secondary antibodies were incubated for 1 h at room temperature. Western blots were developed using chemiluminescence as previously described [19].

2.5. Liquid chromatography–mass spectrometry (LC–MS)

MDA-MB-231 cells were transfected with siControl, siPKM2_1, or siPKM2_2 for 72 h. For metabolite extraction experiments, the transfected cells were washed and exposed to a methanol mixture (methanol:acetonitrile:water, 5:3:2) at 4 °C. After detaching the cells with a cell scraper, the insoluble and soluble materials were separated through centrifugation at 15,000*g* for 15 min (4 °C). Prior to LC–MS analysis, the supernatants were filtered through polytetrafluoroethylene (PTFE) membranes (Millipore, pore size of 0.45 μm) and LC–MS was then performed as previously described [11]. The metabolites were detected with a Thermo Scientific Exactive High-Resolution Mass Spectrometer with electrospray ionization. Identification and quantification of metabolites (phosphoenolpyruvic acid, pyruvate, and lactate) was performed with the LCquan software (Thermo Scientific). Metabolites were positively identified on the basis of exact mass within 5 p.p.m., further validated by concordance with standard retention times and plotted as the peak area for each metabolite [20].

2.6. ATP measurements

MDA-MB-231 cells were transfected with siControl, siPKM2_1, or siPKM2_2 for 72 h. The transfected cells were then washed and lysed using an ATP-release buffer (Sigma, Gillingham, UK). ATP was quantified with an adenosine 5′-triphosphate (ATP) bioluminescent somatic cell assay kit FLASC (Sigma), according to the manufacturer's instructions. For oligomycin experiments, MDA-MB-231 cells were incubated with oligomycin (1 ng/mL) for 24 h prior to ATP measurements. Values were normalized to the total protein content of the cell lysates.

2.7. Quantification of doxorubicin

MDA-MB-231 cells were transfected with siControl, siPKM2_1, or siPKM2_2. After 72 h, the cells were exposed to doxorubicin for 24 h. Cells were then washed and lysed and cell debris was cleared by centrifugation. The supernatant was collected and the drug concentration was measured with high-performance liquid chromatography (HPLC). For the oligomycin experiments, MDA-MB-231 cells were incubated with oligomycin (1 ng/mL) 24 h prior to doxorubicin treatment. The quantity of doxorubicin was normalized against the corresponding protein concentration.

2.8. Tumor model

All animal experiments were performed in compliance with guidelines of the Animal Welfare Act and the guide for the care and use of laboratory animals following protocols approved by the Institutional Animal Care and Use Committee (IACUC). MDA-MB-231 cells were suspended in 40% growth factor reduced matrigel and injected into the mammary fat pad of female Nude mice (Charles River, 4–6 weeks of age, 3×10^6 cells/mouse). The mice were divided into five groups ($n = 8$). The PEI-based delivery system was synthesized and loaded with siRNA as previously described [13–17]. Intravenous administration of doxorubicin (5 mg/kg/week) and siRNAs (20 μg/mouse/week) was initiated when the average tumor volume reached 150–200 mm^3. Tumor volume (V, mm^3) was measured as previously reported ($V = 0.5 \times \text{length} \times \text{width} \times \text{width}$) [21]. To assess the expression of PKM2 in tumor samples, the mice were treated with the indicated therapeutics for four weeks, after which tumor sample were collected 72 h after the final injection.

2.9. Statistical analysis

T-test comparisons (two-tailed, unpaired) were performed to evaluate statistical significance between two groups.

3. Results and discussion

3.1. Effect of PKM2 inhibition on doxorubicin efficacy in vitro

To evaluate the effect of PKM2 inhibition on the therapeutic efficacy of doxorubicin, MDA-MB-231, BT-549, and MDA-MB-436 cells were transfected with two siRNA variants against PKM_2 (siPKM2_1 and siPKM2_2). The ability of the siRNAs to reduce the expression of PKM2 was confirmed with RT-PCR and immunoblotting (Fig. 1A and B). The impact of PKM2 inhibition on doxorubicin efficacy was evident from dose–response curves and IC_{50} values. Namely, the cells lacking PKM2 were more sensitive to doxorubicin treatment (Fig. 1C). We also used another two primary TNBC cell lines (BT-20 and HCC70) to examine the efficacy of doxorubicin in response to PKM2 downregulation. Similar to the above result, the cells following PKM2 inhibition displayed an increased sensitivity to doxorubicin (Fig. S2), indicating that the expression of PKM2 was promoting cell survival during chemotherapeutic stress.

3.2. Effect of PKM2 inhibition on glucose metabolism and ATP production

Since PKM2 is known to play a critical role in the regulation of aerobic glycolysis and ATP production, we hypothesized that PKM2 inhibition would affect glycolysis and ATP levels. The validity of this hypothesis was assessed by measuring the levels of phosphoenolpyruvic acid (PEP), pyruvate, lactate, and ATP in response to PKM2 suppression. As expected, inhibition of PKM2 caused a significant increase in PEP (substrate) levels accompanied by decreased levels of pyruvate (product) and lactate (downstream product), indicating that enzyme activity was successfully suppressed (Fig. 2A–C). Moreover, as a consequence of decreased glycolysis output, the levels of ATP were also reduced in response to treatment (Fig. 2D), providing a possible explanation for siPKM2-induced sensitivity to doxorubicin. Indeed, previous reports have demonstrated that the intracellular levels of ATP in cancer cells correlate with chemotherapeutic sensitivity [22,23].

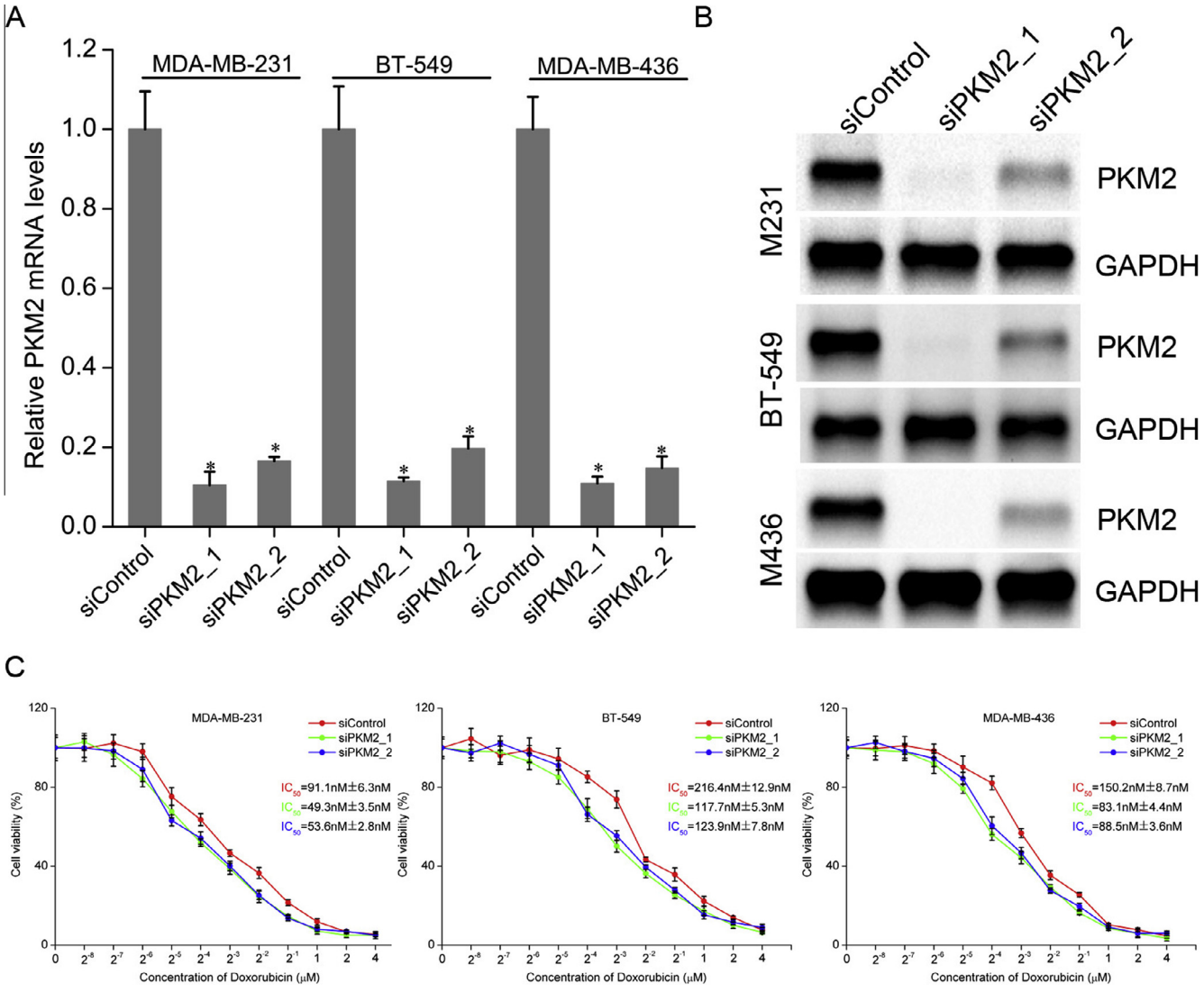

Fig. 1. Suppression of pyruvate kinase isoenzyme M2 (PKM2) in triple-negative breast cancer (TNBC) cells. (A) Messenger RNA (mRNA) levels of PKM2 in MDA-MB-231, BT-549, and MDA-MB-436 cells transfected with siRNAs (siControl, siPKM2_1 or siPKM2_2). (B) Immunoblots from MDA-MB-231 (M231), BT-549, and MDA-MB-436 (M436) cells transfected with siRNAs (siControl, siPKM2_1 or siPKM2_2). Glyceraldehyde 3-phosphate dehydrogenase (GAPDH) was used as a loading control. (C) Relative proliferation and maximal inhibitory concentration (IC_{50}) of doxorubicin in the transfected cells. Data is expressed as mean ± SEM. $^{*}p < 0.05$.

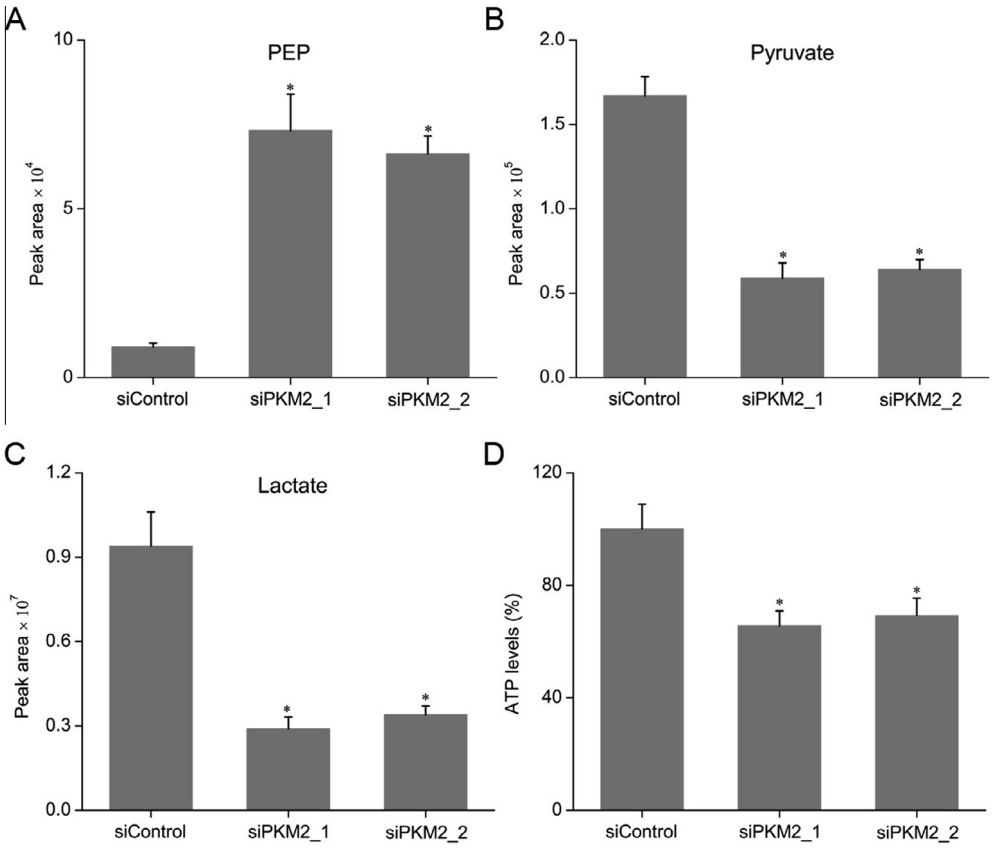

Fig. 2. Effect of PKM2 on glycolysis in MDA-MB-231 cells. (A–C) Levels of intracellular metabolites ((A) phosphoenolpyruvate (PEP); (B) pyruvate; (C) lactate) in siControl, siPKM2_1 and siPKM2_2 treated cells. (D) Intracellular adenosine triphosphate (ATP) levels. Metabolites and ATP levels were normalized to that of the total protein concentration. Data are presented as the mean ± SEM of three samples. $^{*}p < 0.05$.

3.3. Effect of PKM2 inhibition on intracellular accumulation of doxorubicin

Since reduced levels of ATP have been found to increase chemotherapeutic efficacy, we speculated that this effect could be attributed to ATP-dependent membrane pumps, including the p-glycoprotein 1 (P-gp) encoded by the multidrug resistance protein 1 (MRP1) [22,23]. Namely, decreased levels of ATP would impair the activity of such pumps, resulting in increased intracellular accumulation of chemotherapeutics. To examine whether the siPKM2-induced reduction in ATP could impact the intracellular accumulation of doxorubicin, the relative quantities of doxorubicin were measured in MDA-MB-231 cells. Cells lacking PKM2 expression displayed elevated levels of intracellular doxorubicin compared to cells treated with siControl (Fig. 3A). The mitochondrial ATP synthase inhibitor oligomycin was used to confirm that the increased accumulation of doxorubicin was due to reduced levels of ATP, as opposed to other effects of PKM2 inhibition. Indeed, oligomycin administration resulted in higher concentrations of intracellular doxorubicin and improved therapeutic efficacy (Fig. 3B and C). Taken together, these results suggest that siPKM2 can sensitize cells to doxorubicin by impeding ATP production, consequently elevating intracellular levels of doxorubicin.

3.4. Effect of PKM2 inhibition on doxorubicin efficacy in vivo

Given that the inhibition of PKM2 enhanced the anticancer activity of doxorubicin in cell culture, the effect of siPKM2 was further assessed *in vivo*. The therapeutic efficacy of combinational treatment with siPKM2 and doxorubicin was evaluated in an orthotopic mouse model of MDA-MB-231 breast cancer. PKM2 siRNA was systemically delivered using a PEI-based delivery system, as previously described [13–17]. The ability of the siRNA carrier to decrease PKM2 protein levels in tumor samples was evaluated by immunohistochemistry and immunoblotting. The results show a substantial reduction in PKM2 levels in mice treated with the PEI vector containing siPKM2 (Fig. 4A and B), demonstrating the successful *in vivo* delivery of siRNA to cancer cells. Notably, in accordance with the *in vitro* results, doxorubicin displayed a more pronounced inhibition of tumor growth in mice that were simultaneously treated with siPKM2_1 (Fig. 4C), providing further evidence that PKM2 inhibition can enhance the efficacy of doxorubicin. Moreover, the results demonstrate that PKM2 inhibition in the absence of doxorubicin did not have an effect on tumor growth (Fig. 4C). This observation is in agreement with previous study showing that short hairpin RNA (shRNA) against PKM2 was unable to halt breast cancer progression *in vivo* [24]. However, there is evidence that PKM2 plays a role during tumor initiation [7,12], suggesting that PKM2 is important during the initial stages of breast cancer formation, but is not required for maintaining tumor growth. In this study, siPKM2 treatment was initiated after tumors had passed the early stages of development.

In summary, we demonstrate that siRNA-mediated suppression of PKM2 enhances the *in vitro* and *in vivo* anticancer efficacy of doxorubicin. The proposed mechanism is that of PKM2-induced inhibition of glycolysis, which results in decreased ATP levels and increased intracellular accumulation of doxorubicin. These results indicate that PKM2 could be a promising therapeutic target for

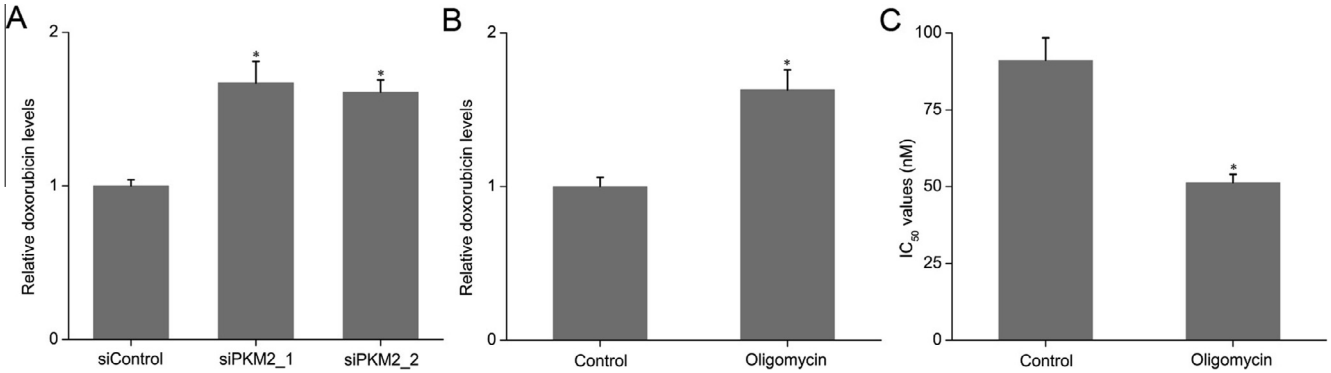

Fig. 3. Effect of PKM2 inhibition on the intracellular level of doxorubicin in MDA-MB-231 cells. (A) Intracellular levels of doxorubicin in cells transfected with siControl, siPKM2_1 or siPKM2_2. (B) Intracellular levels of doxorubicin measured in the absence or presence of oligomycin. (C) IC_{50} values of doxorubicin in the absence or presence of oligomycin. The data are presented as the mean ± SEM of tree samples. $^{*}p < 0.05$.

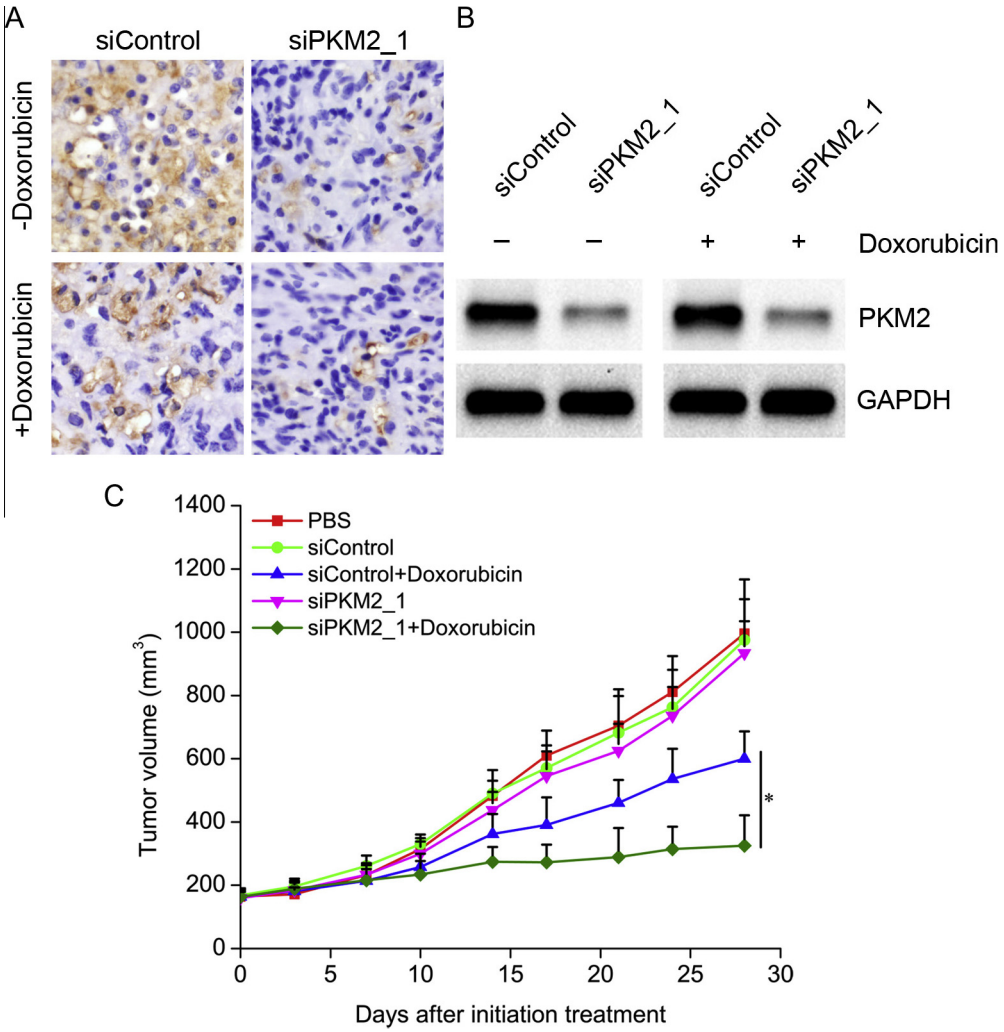

Fig. 4. Combinational treatment of doxorubicin and siPKM2 in an orthotopic MDA-MB-231 tumor model. (A) Immunohistochemical analysis of PKM2 expression in tumor tissues. Nuclei, blue; PKM2-specific horseradish peroxidase (HRP) signal, brown. (B) Western blot analysis of PKM2 expression in tumor tissues. (C) Tumor volume in response to treatment. Statistical comparisons were made between the target siPKM2_1 + doxorubicin group and the siControl + doxorubicin group. The results are expressed as the mean ± SEM. $^{*}p < 0.05$. (For interpretation of the references to color in this figure legend, the reader is referred to the web version of this article.)

enhancing the anticancer activity of doxorubicin in patients with TNBC. The development of strategies for improving the outcome of conventional chemotherapeutic agents is especially important for TNBC, due to few available treatment options and a high prevalence of drug resistance.

Acknowledgment

The authors acknowledge supports from the following funding source: Excellent Academic Backbone Program of Tenth People's Hospital of Shanghai (No. 12XSGG102).

Appendix A. Supplementary data

Supplementary data associated with this article can be found, in the online version, at http://dx.doi.org/10.1016/j.bbrc.2014.10.109.

References

[1] S. Cleator, W. Heller, R.C. Coombes, Triple-negative breast cancer: therapeutic options, Lancet Oncol. 8 (2007) 235–244.
[2] M.J. Duffy, P.M. McGowan, J. Crown, Targeted therapy for triple-negative breast cancer: where are we?, Int J. Cancer 131 (2012) 2471–2477.
[3] B. Weigelt, J.S. Reis, Histological and molecular types of breast cancer: is there a unifying taxonomy?, Nat Rev. Clin. Oncol. 6 (2009) 718–730.
[4] S.J. Isakoff, Triple-negative breast cancer: role of specific chemotherapy agents, Cancer J. 16 (2010) 53–61.
[5] I.J. Bristol, W.A. Woodward, E.A. Strom, M. Cristofanilli, D. Domain, S.E. Singletary, G.H. Perkins, J.L. Oh, T.K. Yu, W. Terrefe, A.A. Sahin, K.K. Hunt, G.N. Hortobagyi, T.A. Buchholz, Locoregional treatment outcomes after multimodality management of inflammatory breast cancer, Int. J. Radiat. Oncol. Biol. Phys. 72 (2008) 474–484.
[6] K. Gelmon, R. Dent, J.R. Mackey, K. Laing, D. McLeod, S. Verma, Targeting triple-negative breast cancer: optimising therapeutic outcomes, Ann. Oncol. 23 (2012) 2223–2234.
[7] H.R. Christofk, M.G. Heiden, M.H. Harris, A. Ramanathan, R.E. Gerszten, R. Wei, M.D. Fleming, S.L. Schreiber, L.C. Cantley, The M2 splice isoform of pyruvate kinase is important for cancer metabolism and tumour growth, Nature 452 (2008) 230–233.
[8] W.J. Israelsen, T.L. Dayton, S.M. Davidson, B.P. Fiske, A.M. Hosios, G. Bellinger, J. Li, Y. Yu, M. Sasaki, J.W. Horner, L.N. Burga, J. Xie, M.J. Jurczak, R.A. DePinho, C.B. Clish, T. Jacks, R.G. Kibbey, G.M. Wulf, D. Di Vizio, G.B. Mills, L.C. Cantley, M.G. Vander Heiden, PKM2 isoform-specific deletion reveals a differential requirement for pyruvate kinase in tumor cells, Cell 155 (2013) 397–409.
[9] R. Possemato, K.M. Marks, Y.D. Shaul, M.E. Pacold, D. Kim, K. Birsoy, S. Sethumadhavan, H.K. Woo, H.G. Jang, A.K. Jha, W.W. Chen, F.G. Barrett, N. Stransky, Z.Y. Tsun, G.S. Cowley, J. Barretina, N.Y. Kalaany, P.P. Hsu, K. Ottina, A.M. Chan, B. Yuan, L.A. Garraway, D.E. Root, M. Mino-Kenudson, E.F. Brachtel, E.M. Driggers, D.M. Sabatini, Functional genomics reveal that the serine synthesis pathway is essential in breast cancer, Nature 476 (2011) 346–350.
[10] H.R. Christofk, M.G. Vander Heiden, N. Wu, J.M. Asara, L.C. Cantley, Pyruvate kinase M2 is a phosphotyrosine-binding protein, Nature 452 (2008) 181–186.
[11] B. Chaneton, P. Hillmann, L. Zheng, A.C. Martin, O.D. Maddocks, A. Chokkathukalam, J.E. Coyle, A. Jankevics, F.P. Holding, K.H. Vousden, C. Frezza, M. O'Reilly, E. Gottlieb, Serine is a natural ligand and allosteric activator of pyruvate kinase M2, Nature 491 (2012) 458–462.
[12] M.S. Goldberg, P.A. Sharp, Pyruvate kinase M2-specific siRNA induces apoptosis and tumor regression, J. Exp. Med. 209 (2012) 217–224.
[13] B. Urban-Klein, S. Werth, S. Abuharbeid, F. Czubayko, A. Aigner, RNAi-mediated gene-targeting through systemic application of polyethylenimine (PEI)-complexed siRNA *in vivo*, Gene Ther. 12 (2005) 461–466.
[14] M. Grzelinski, B. Urban-Klein, T. Martens, K. Lamszus, U. Bakowsky, S. Hobel, F. Czubayko, A. Aigner, RNA interference-mediated gene silencing of pleiotrophin through polyethylenimine-complexed small interfering RNAs *in vivo* exerts antitumoral effects in glioblastoma xenografts, Hum. Gene Ther. 17 (2006) 751–766.
[15] Y. Wang, P. Chen, J. Shen, The development and characterization of a glutathione-sensitive cross-linked polyethylenimine gene vector, Biomaterials 27 (2006) 5292–5298.
[16] U. Lungwitz, M. Breunig, T. Blunk, A. Gopferich, Polyethylenimine-based non-viral gene delivery systems, Eur. J. Pharm. Biopharm. 60 (2005) 247–266.
[17] M. Gunther, J. Lipka, A. Malek, D. Gutsch, W. Kreyling, A. Aigner, Polyethylenimines for RNAi-mediated gene targeting *in vivo* and siRNA delivery to the lung, Eur. J. Pharm. Biopharm. 77 (2011) 438–449.
[18] F. Wang, Y. Yang, Identification of an antitumor immune response of polyhistidine through a toll-like receptor 4-dependent manner, Biochem. Biophys. Res. Commun. 453 (2014) 148–152.
[19] F. Wang, Y. Yang, Quercetin suppresses insulin receptor signaling through inhibition of the insulin ligand-receptor binding and therefore impairs cancer cell proliferation, Biochem. Biophys. Res. Commun. 452 (2014) 1028–1033.
[20] O.D.K. Maddocks, C.R. Berkers, S.M. Mason, L. Zheng, K. Blyth, E. Gottlieb, K.H. Vousden, Serine starvation induces stress and p53-dependent metabolic remodelling in cancer cells, Nature 493 (2013) 542–546.
[21] F. Wang, Y. Yang, Suppression of the xCT-CD44v antiporter system sensitizes triple-negative breast cancer cells to doxorubicin, Breast Cancer Res. Treat. 147 (2014) 203–210.
[22] M.M. Gottesman, T. Fojo, S.E. Bates, Multidrug resistance in cancer: role of ATP-dependent transporters, Nat. Rev. Cancer 2 (2002) 48–58.
[23] A. Garnier-Suillerot, C. Marbeuf-Gueye, M. Salerno, C. Loetchutinat, I. Fokt, M. Krawczyk, T. Kowalczyk, W. Priebe, Analysis of drug transport kinetics in multidrug-resistant cells: implications for drug action, Curr. Med. Chem. 8 (2001) 51–64.
[24] M. Cortes-Cros, C. Hemmerlin, S. Ferretti, J. Zhang, J.S. Gounarides, H. Yin, A. Muller, A. Haberkorn, P. Chene, W.R. Sellers, F. Hofmann, M2 isoform of pyruvate kinase is dispensable for tumor maintenance and growth, Proc. Natl. Acad. Sci. U.S.A. 110 (2013) 489–494.